On the Influence of Microphone Array Geometry on the Behavior of Hypercomplex Adaptive Filters

Francesca Ortolani, Michele Scarpiniti, Danilo Comminiello and Aurelio Uncini
Dpt. of Information Engineering, Electronics and Telecommunications
Sapienza University of Rome, Rome, Italy
francesca.ortolani, michele.scarpiniti, danilo.comminiello, aurelio.uncini@uniroma1.it

***Abstract*—The performance of hypercomplex adaptive filters has been widely experimented during the last decade. Quaternion filters, especially, have been utilized in systems where the signals to be processed have some form of correlation. However, besides correlation, some resolved explanation about what particular algebra to use in a certain context has not been provided, yet. This work tries to contribute in this direction by proposing an experiment that puts filters to the test with changing the input signal geometry. The tests presented in this paper take place in acoustic environment and show how a proper sound space transformation, along with the choice of the mathematical format for processing, can improve a filter performance.**

Keywords—Ambisonics; Coincident arrays; Hypercomplex; Multidimensional Signal Processing; Quaternions; Spaced arrays; Tessarines

I. INTRODUCTION

The captivating side of hypercomplex algebras attracted scientists and encouraged the world of research to uncover the environments and the circumstances in which the application of hypercomplex numbers finds fertile ground. After the initial definition of these new numerical systems [1–4] a wave of study touched physics and the description of classical problems [5]. The simplest mathematical objects after complex numbers are quaternions [1]. The compact formalism provided by quaternion maths achieved resounding success and many 3-D problems in physics and their laws were reformulated in a quaternion fashion, e.g. Maxwell's equations of electromagnetism [6], Newton's laws of motion [7], gravity [8], quantum mechanics and the electron wave theory [9], etc. The new formalism surely simplified the expression and the divulgation of many scientific theories among insiders. Nevertheless, considered that these hypercomplex algebras may not be easily understandable for those people having an unspecialized knowledge of mathematics, soon a question arose: do we really need quaternions and octonions? Probably, the answer arrived from the world of engineering. The challenge has been the provision of convincing reasons why hypercomplex signal processing is favorable (or not). It is known that the orientation information is intrinsic to quaternion-valued objects [10]. Therefore, quaternions found a new revival in 3-D rotation applications. These include avionics, 3-D graphics and virtual reality, modeling in chemistry, etc. The experimentation of quaternion algebra and the implementation of quaternion systems determined a first motivation why quaternions are irreplaceable in these fields: before quaternions, all rotations were traditionally expressed in Euler angles. Unfortunately, such a representation is affected by system deadlocks occurring at critical angles. Practically, the rotation system may degenerate and lose a degree of freedom. Other positive impressions of hypercomplex algebras originated from quaternion adaptive signal processing. Adaptive filters are self-adjusting systems, so human intervention is restricted to the filter development and parameter setup phases. It has been interesting to study how such *automatic* systems behave with changing the mathematical format of input and output signals and the filter architecture, accordingly. It was experimented that signal component correlation plays a significant role in the adaptation process, thus speeding up the convergence rate and improving the filter performance. On this trend, researchers developed several algorithms in quaternion algebra [11–15]. Our research group also dedicated itself to this topic [16, 17]. The aim of this paper is to continue the research presented in a previous work. In [17], the authors experimented whether a certain numerical representation of the sound space can determine a filter performance. The test compared the filter convergence rate in the case the input signal components were totally uncorrelated and unstructured or correlated and in a format derived from a 3-D audio technique called *Ambisonics*. Both system configurations had four signal components. For this reason, the tests were carried out in two 4-dimensional algebras: quaternion and tessarine algebras. The authors compared the performance of two elementary isodimensional Least Mean Square (LMS) adaptive filters: the Quaternion LMS (QLMS) and the Tessarine LMS (TLMS). In the case of complete decorrelation and absence of structure, the TLMS and the QLMS exhibit the same behavior. Things change when the system has a determined geometry and correlated component signals. In fact, the QLMS algorithm converges faster when the input signal has the Ambisonic format. Here in this work, we still keep four signals and correlation of components, but we change the microphone layout. We will repeat the same experiment proposed in [17] and compare the filter performance in the case a coincident Ambisonic array or a 4-element uniform linear array is used. The aim of our new experiment is to assess whether mere correlation is dominant over geometry.

This paper is organized as follows. After a preliminary introduction to 4-dimensional algebras in Section II, the two different microphone geometries are presented in Section III and a brief recap of the QLMS and TLMS algorithms is supplied in Section IV. Finally, results from simulations are reported in Section V.

II. Two 4-dimensional algebras

Two 4-dimensional algebras are presented here: quaternions ($\mathbb{H}$) and tessarines ($\mathbb{T}$). Other 4-D algebras exist, e.g. the Sklyanin algebras described in [18]; however, we chose these two algebras because they are characterized by the fact that their *outfit* is exactly the same: $q = q_0 + q_1\mathbf{i} + q_2\mathbf{j} + q_3\mathbf{k}$ with $q \in \mathbb{H}$ and $t = t_0 + t_1\mathbf{i} + t_2\mathbf{j} + t_3\mathbf{k}$ with $t \in \mathbb{T}$. Despite that, the algebraic rules governing quaternion and tessarine algebras are radically different. Both quaternions and tessarines can be split into a real (scalar) part (i.e. q_0 and t_0), and a full-imaginary (vector) part built on the imaginary axes $\mathbf{i}, \mathbf{j}, \mathbf{k}$. The properties below are those responsible of the essential differences between quaternion and tessarine numerical systems:

Quaternion algebra:

$$\mathbf{ij} = \mathbf{k}, \quad \mathbf{jk} = \mathbf{i}, \quad \mathbf{ki} = \mathbf{j}, \tag{1}$$

$$\mathbf{i}^2 = \mathbf{j}^2 = \mathbf{k}^2 = -1. \tag{2}$$

Tessarine algebra:

$$\mathbf{ij} = \mathbf{k}, \quad \mathbf{jk} = \mathbf{i}, \quad \mathbf{ki} = -\mathbf{j}, \tag{3}$$

$$\mathbf{i}^2 = \mathbf{k}^2 = -1, \mathbf{j}^2 = +1. \tag{4}$$

Axioms **Ошибка! Источник ссылки не найден.**– □4□ generate the discrepancies between the two algebras, e.g. they dictate the rules for product and other mathematical operations (convolution, correlation, etc.).

Given quaternions $q_a, q_b \in \mathbb{H}$, we compute their product as

$$\begin{aligned} q_a q_b &= (a_0 + a_1\mathbf{i} + a_2\mathbf{j} + a_3\mathbf{k})(b_0 + b_1\mathbf{i} + b_2\mathbf{j} + b_3\mathbf{k}) \\ &= (a_0 b_0 - a_1 b_1 - a_2 b_2 - a_3 b_3) \\ &+ (a_0 b_1 + a_1 b_0 + a_2 b_3 - a_3 b_2)\mathbf{i} \\ &+ (a_0 b_2 - a_1 b_3 + a_2 b_0 + a_3 b_1)\mathbf{j} \\ &+ (a_0 b_3 + a_1 b_2 - a_2 b_1 + a_3 b_0)\mathbf{k}. \end{aligned} \tag{5}$$

Given tessarines $t_a, t_b \in \mathbb{T}$, we compute their product as

$$\begin{aligned} t_a t_b &= (a_0 + a_1\mathbf{i} + a_2\mathbf{j} + a_3\mathbf{k})(b_0 + b_1\mathbf{i} + b_2\mathbf{j} + b_3\mathbf{k}) \\ &= (a_0 b_0 - a_1 b_1 + a_2 b_2 - a_3 b_3) \\ &+ (a_0 b_1 + a_1 b_0 + a_2 b_3 + a_3 b_2)\mathbf{i} \\ &+ (a_0 b_2 - a_1 b_3 + a_2 b_0 - a_3 b_1)\mathbf{j} \\ &+ (a_0 b_3 + a_1 b_2 + a_2 b_1 + a_3 b_0)\mathbf{k}. \end{aligned} \tag{6}$$

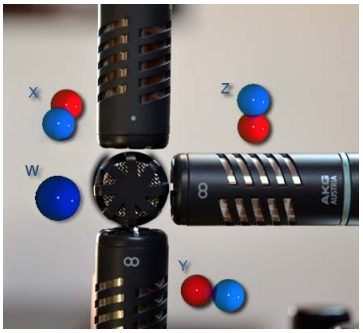

Fig. 1. Typical Ambisonic B-Format layout.

Fig. 2. 4-Microphone Uniform Linear Array**.**

It can be seen that commutativity features only in tessarine algebra. As a consequence of this, for example, we can detect an effect on the convolution theorem. In fact, the classic convolution theorem (valid in $\mathbb{R}$, $\mathbb{C}$) does not hold in quaternion algebra [16,19]. On the contrary, the authors of this paper experimented that the theorem is still valid in tessarine algebra. This result will be reported in a future work. On the other hand, the sum is computed the same way with either quaternions or tessarines (component-by-component):

$$\begin{aligned} q \pm p &= (q_0 + q_1\mathbf{i} + q_2\mathbf{j} + q_3\mathbf{k}) \pm (p_0 + p_1\mathbf{i} + p_2\mathbf{j} + p_3\mathbf{k}) \\ &= (q_0 \pm p_0) + (q_1 \pm p_1)\mathbf{i} + (q_2 \pm p_2)\mathbf{j} + (q_3 \pm p_3)\mathbf{k}. \end{aligned} \tag{7}$$

Another consequence of the divergent algebraic background is the distinct definition of the conjugate of a quaternion and a tessarine:

$$\begin{aligned} q^* &= q_0 - q_1\mathbf{i} - q_2\mathbf{j} - q_3\mathbf{k} \in \mathbb{H} \\ t^* &= t_0 - t_1\mathbf{i} + t_2\mathbf{j} - t_3\mathbf{k} \in \mathbb{T} \end{aligned} \tag{8}$$

However, the *poly-conjugation* can generalize both:

$$p^* = p_0 + \sum_{\nu=1}^{3} p_\nu \mathbf{e}_\nu^3 \tag{9}$$

where $\mathbf{e}_\nu$ with $\nu = 1, 2, 3$ form an orthonormal basis.

III. Microphone Array geometries and Mathematical Representation of Space

The experiment we are going to present in this paper makes use of two different microphone configurations to pick up a sound source. Both layouts mount four microphones and each microphone signal is assigned to a quaternion/tessarine

component. The first microphone configuration is a coincident array, extensively used in the so-called *Ambisonics (1st order) B-format* technique (Fig. 1). The second is a simple 4-element uniform linear array (Fig. 2).

Besides the evident different shape of the arrays, a transformation of the sound space is applied before placing each signal into a mathematical dimension. Details about this transformation are given just below.

A. Ambisonic Coincident Array

Ambisonics is a renowned 3-D audio technique patented in the '70s by Gerzon and Felgett [20–22]. This technique can be used for either recording or reconstructing a 3-dimensional sound field. Ambisonics typically uses coincident microphone arrays with a configuration depending on the specific *format*. Ambisonic formats were tailored to a special audio equipment or purpose (studio recording, audio broadcasting, public address, etc.) and it is possible to transcode from one format to another by means of uncomplicated matrix transformations [23]. We will focus here on the Ambisonic *B-Format*. The choice and the arrangement of the microphones in this format are in line with the physical decomposition of the sound field according to the Ambisonic theory. Ambisonics describes the sound field, $p(\vec{r})$, as a linear combination of *spherical harmonics* (Y_{mn}^{σ}), multiplied by coefficients representing the recorded audio signals (B_{mn}^{σ}):

$$p(\vec{r}) = \sum_{m=0}^{\infty} (2m+1)\, j^m J_m(kr) \sum_{\substack{0\le n\le m \\ \sigma=\pm 1}} B_{mn}^{\sigma} Y_{mn}^{\sigma}(\theta,\varphi) \quad (10)$$

where m, n, σ, k are the degree, the order, the spin and the wave number ($2\pi f/c$), respectively. The polar coordinates (θ,φ) denote the azimuth and the elevation. The decomposition in (10) refers to a plane wave and a sound field with external sources only. The other functions in the formula, $J_m(kr)$, are radial functions called *spherical Bessel functions of the first kind* [24]. The *1st-order B-Format* considers harmonics up to first order. Graphically, the zeroth and first order harmonics are represented by the colored bubbles in Fig. 1. The microphones used with this technique (coincident and orthogonal to one another) must have polar patterns fitting the shape of these harmonics. For this reason, one omnidirectional microphone (W) and three figure-of-eight microphones (X,Y,Z) are adopted here.

A transformation of the sound field from the traditional Euler representation into a quaternion-valued form has been already discussed and experimented by the authors of this paper [17, 25, 26]. The group of 3-D Euclidean rotations SO(3) has a representation on the $(2m+1)$–dimensional Hilbert space with spherical harmonics, $span\{Y_{mn}^{\sigma}(\theta,\varphi), 0 \le n \le m, \sigma = \pm 1\}$. In addition, the SO(3) group is isomorphic to the subspace of full-imaginary quaternions. That said, the transformation is possible and straightforward, as indicated in Table 1. In conclusion, 1st-order B-format can be condensed into a quaternion form as

$$B^{Q}(t) = B_W(t) + B_X(t)\mathbf{i} + B_Y(t)\mathbf{j} + B_Z(t)\mathbf{k}. \quad (11)$$

Later in this work, we will see if a similar transformation is effective in tessarine mathematics, too.

B. Uniform Linear Array

The second microphone configuration we present here consists of four uniformly spaced microphones, aligned on a single space dimension (Fig. 2). The microphone polar pattern may be of any kind. It is preferable that all microphones have the same directional characteristic. Such arrays are usually employed in highly directive beamforming applications, such as sound source localization. System directivity depends on the number of sensors, their spacing and the wavelength of the impinging wave.

TABLE I. SPHERICAL HARMONICS UP TO 1ST ORDER: EULER TO QUATERNION

Ord.	m,n,σ	Ch.	Euler Spherical Harmonics (normalized)	Quaternion Spherical Harmonics
0	0,0,1	W	1	1
1	1,1,1	X	$\cos\theta\cos\varphi$	$x\mathbf{i}$
1	1,0,1	Z	$\sin\varphi$	$z\mathbf{k}$
1	1,1,-1	Y	$\sin\theta\cos\varphi$	$y\mathbf{j}$

The spatial position of each microphone in our 4-element array is defined as

$$r_p = [(p-1)d \;\; 0 \;\; 0]^T, \quad \text{for } p = 1,\ldots,P \quad (12)$$

where d is the distance between two microphones and $\mathrm{P} = 4$. In a uniform linear array (ULA) the delay time between sensors is $\tau = d\cos\theta/c$, where θ is the angle of incidence of the acoustic wave. The ULA array steering vector can be expressed as

$$\mathbf{a} = \left[1 \;\; e^{jkd\cos\theta} \;\; \ldots \;\; e^{j(1-P)kd\cos\theta}\right]^T \quad (13)$$

with $\mathrm{P} = 4$ and $k = \omega / c$ (c is the speed of sound).

Given the source signal $s(t)$, the sound signal at the p-th microphone can be represented as

$$x_p(t) = s(t-(p-1)\tau) \quad (14)$$

Since we have four microphone signals and they are correlated to one another, we may want to assign each signal to a quaternion or a tessarine component. No particular space transformation is applied here. We are just encapsulating signals into one single multidimensional object, because they belong to the same context:

$$x^{Q,T}(t) = x_1(t) + x_2(t)\mathbf{i} + x_3(t)\mathbf{j} + x_4(t)\mathbf{k}. \quad (15)$$

IV. A COMPARISON OF 4-D ADAPTIVE FILTERS

In quaternion algebra, the development of adaptive filters has been progressing for about a decade. Since the first Quaternion Least Mean Square algorithm was presented in [11], improvements and other quaternion algorithm architectures were proposed. On the contrary, tessarine algebra did not arise the same interest as quaternions, so the literature lacks of filters in this algebra. On account of this, the authors of this paper implemented the basic Tessarine LMS algorithm in order to make a comparison with its quaternion counterpart [17]. The main information about the basic LMS algorithm is provided in the following.

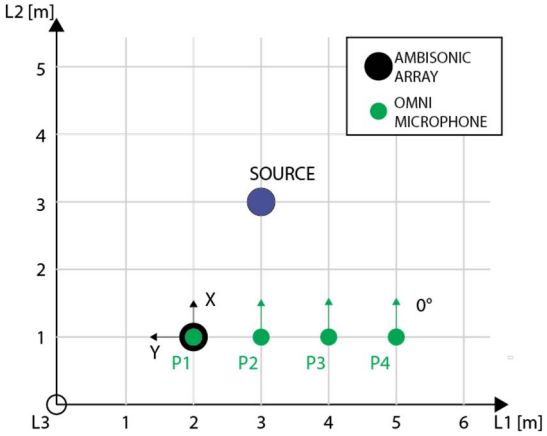

Fig. 3. Simulation room scenario.

In the LMS adaptation process we define a cost function to be minimized, e.g. the Mean Square Error (MSE) $J_n(\mathbf{w}_n) = E\{e[n]e^*[n]\}$. The error $e[n]$ is measured as the difference between a desired signal and the adaptive filter output ($e[n] = d[n] - y[n]$). Considering the properties of quaternion and tessarine algebras, the adaptive filter output is slightly different in the two algebras:

$$y[n] = \mathbf{w}_{n-1}^T \mathbf{x}_n = \begin{bmatrix} \mathbf{w}_a^T\mathbf{x}_a - \mathbf{w}_b^T\mathbf{x}_b - \mathbf{w}_c^T\mathbf{x}_c - \mathbf{w}_d^T\mathbf{x}_d \\ \mathbf{w}_a^T\mathbf{x}_b + \mathbf{w}_b^T\mathbf{x}_a + \mathbf{w}_c^T\mathbf{x}_d - \mathbf{w}_d^T\mathbf{x}_c \\ \mathbf{w}_a^T\mathbf{x}_c + \mathbf{w}_c^T\mathbf{x}_a + \mathbf{w}_d^T\mathbf{x}_b - \mathbf{w}_b^T\mathbf{x}_d \\ \mathbf{w}_a^T\mathbf{x}_d + \mathbf{w}_d^T\mathbf{x}_a + \mathbf{w}_b^T\mathbf{x}_c - \mathbf{w}_c^T\mathbf{x}_b \end{bmatrix} \in \mathbb{H} \quad (16)$$

for quaternions, and

$$y[n] = \mathbf{w}_{n-1}^T \mathbf{x}_n = \begin{bmatrix} \mathbf{w}_a^T\mathbf{x}_a - \mathbf{w}_b^T\mathbf{x}_b + \mathbf{w}_c^T\mathbf{x}_c - \mathbf{w}_d^T\mathbf{x}_d \\ \mathbf{w}_a^T\mathbf{x}_b + \mathbf{w}_b^T\mathbf{x}_a + \mathbf{w}_c^T\mathbf{x}_d + \mathbf{w}_d^T\mathbf{x}_c \\ \mathbf{w}_a^T\mathbf{x}_c + \mathbf{w}_c^T\mathbf{x}_a - \mathbf{w}_d^T\mathbf{x}_b - \mathbf{w}_b^T\mathbf{x}_d \\ \mathbf{w}_a^T\mathbf{x}_d + \mathbf{w}_d^T\mathbf{x}_a + \mathbf{w}_b^T\mathbf{x}_c + \mathbf{w}_c^T\mathbf{x}_b \end{bmatrix} \in \mathbb{T} \quad (17)$$

for tessarines, where $\mathbf{x}_n$ is the filter input vector at iteration n and $\mathbf{w}_{n-1}$ are the filter weights at iteration $n-1$: $\mathbf{x}_n = [x[n]\ x[n-1]\ \dots\ x[n-M]]^T$, $\mathbf{w}_n = [w_0[n]\ w_1[n]\ \dots\ w_M[n]]^T$ with M the filter length. The minimum of the cost function $J_n(\mathbf{w}_n)$ can be found by computing and setting to zero its gradient. The final adaptation equation for both QLMS and TLMS algorithms results in

$$\mathbf{w}_n = \mathbf{w}_{n-1} + \mu e[n]\mathbf{x}_n^*. \quad (18)$$

where μ is the step size along the direction of the gradient and the conjugate $\mathbf{x}_n^*$ is derived as in (9).

The QLMS and the TLMS algorithms will be employed in the simulations described in Section V.

V. SIMULATIONS

As introduced, we are going to repeat the experiment proposed by the authors in [17]. In this work, we chose two different microphone configurations having a precise geometry. The microphones are set up as described in Section III-A and Section III-B. The ULA array is composed of omnidirectional microphones. The four signal components are correlated in both cases. The positions of the source and the microphones in the room are described in Fig. 3. The resulting impulse responses, characterizing the path between the source and each sensor, in the case of Ambisonics and ULA are reported in Fig. 4 and Fig. 5, respectively.

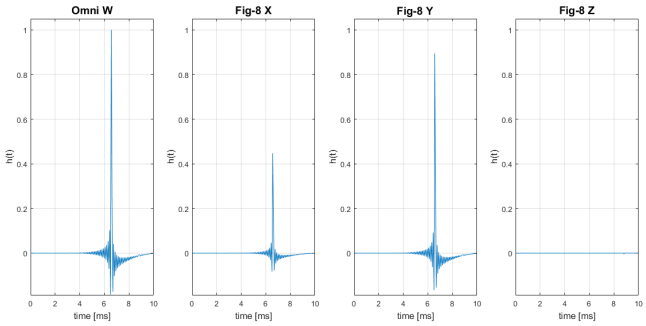

Fig. 4. B-Format impulse responses.

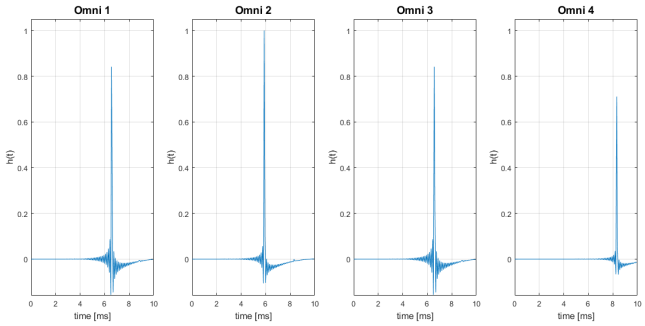

Fig. 5. Uniform Linear Array impulse responses (omnidirectional mics).

The experiment consists in the identification of a 4-dimensional system, previously defined in the time domain by the random weights $\mathbf{w}_0$, uniformly distributed in the range $[-1,1]$. The adaptive core accomplishing this task is one of the algorithms presented in Section IV. The filter input is recorded in the two techniques. The source generates unit-variance white

Gaussian noise. Given the same filter parameters for both QLMS and TLMS ($M = 12$, $\mu = 0.8$), we obtained the results plotted in Fig. 6 and Fig. 7 with B-Format and ULA, respectively. We considered as a measure of comparison the MSE at the steady-state and the time (in terms of samples) the algorithm takes to reach this value.

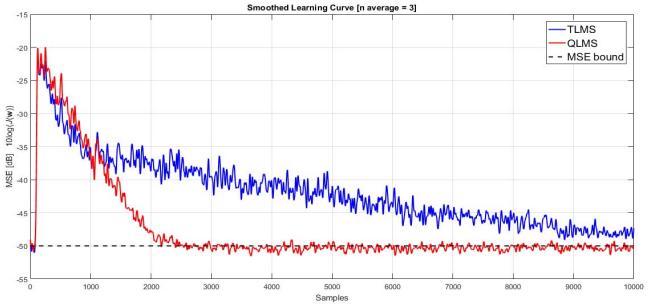

Fig. 6. System identification with B-Format input signal. QLMS and TLMS filter performance.

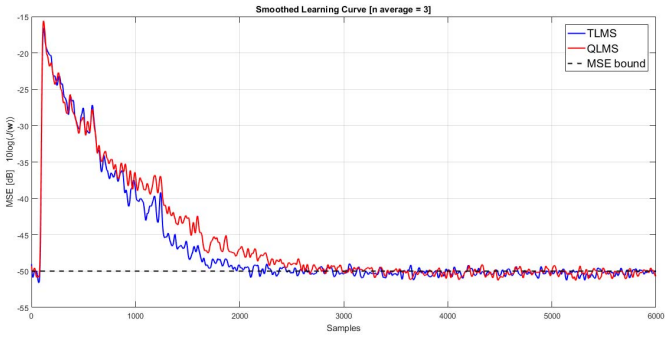

Fig. 7. System identification with ULA (omnidirectional mics) input signal. QLMS and TLMS filter performance.

In both cases, the QLMS has an edge over TLMS. However, when the input signal is consistent with the quaternion transformation we discussed in Section III-A, this advantage is distinct. Apparently, a similar transformation is not feasible with tessarines, since, unlike rotations and quaternions, tessarine algebra is commutative. In the example above, geometry wins over mere correlation. Nevertheless, we are interested in observing whether it is possible to turn the situation around. We present here a minor modification of the scenario. Keeping the position of microphone P1 unchanged, the omnidirectional ULA microphones are moved closer to one another ($d = 0.5$ [m]). The impulse responses are shown in Fig. 8 and the result from the simulation is plotted in Fig. 9. Here, the TLMS converges faster than the QLMS. In conclusion, correlation matters, but geometry is preponderant. In fact, geometry implies a particular configuration of correlation.

VI. Conclusion

In this paper, we have investigated the effect of the microphone array layout in combination with the mathematical description of the surrounding environment on the performance of adaptive filters. We made use of a coincident array and a uniform linear array of microphones, both of them made up of four elements. We have transformed the sound space into a 4-dimensional format and we have applied the resulting multidimensional signal to 4-dimensional adaptive filters (QLMS and TLMS). We have seen that, in the special case the

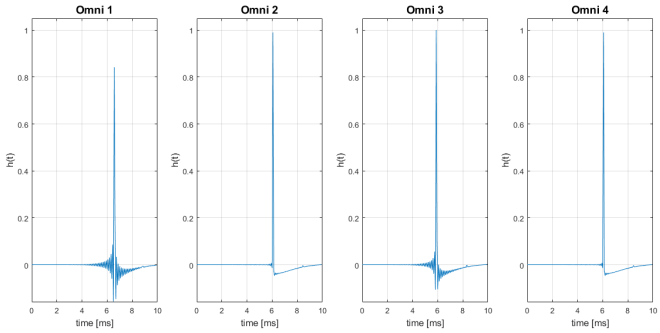

Fig. 8. Uniform Linear Array impulse responses (closer omni mics).

space is decomposed into spherical harmonics and the Ambisonic B-Format technique is used to record the sound field, the choice of quaternion algebra in signal processing works like the right key in the lock. In this instance, the QLMS algorithm converges faster than the TLMS algorithm. The outcome of this test suggests that, in this special context, quaternion algebra is a better choice. In the case signals are simply correlated, but the sound space does not undergo any special transformation, there may be still an advantage of quaternion signal processing over tessarine algebra, although not so evident. In fact, we have seen how changing the distance between the microphones overturned the result. Further investigation is totally required.

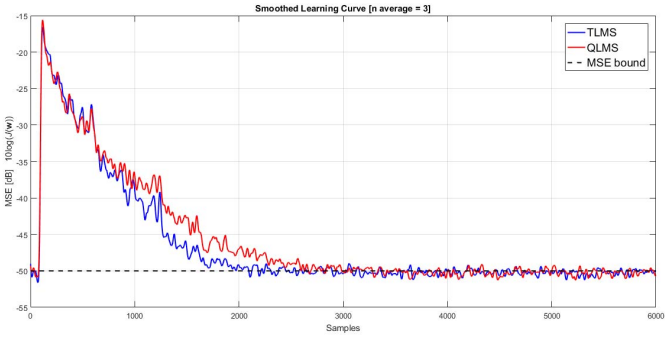

Fig. 9. System identification with ULA (closer omni mics) input signal. QLMS and TLMS filter performance.

References

[1] W. R. Hamilton, Elements of Quaternions. Longmans, Green & Co., 1866.

[2] A. Cayley and A. R. Forsyth, The collected mathematical papers of Arthur Cayley. Cambridge University Press, 1889.

[3] S. Lie, “Über complexe, insbesondere linien- und kugel-complexe, mit anwendung auf die theorie partieller differentialgleichungen,” Math. Ann., vol. 5, pp. 145–208, 1872.

[4] J. C. Baez, “The octonions,” Bull. Amer. Math. Soc., vol. 39, no. 2, pp. 145–205, 2001.

[5] “Number, geometry and nature,” Hypercomplex Numbers in Geometry and Physics, vol. 1, no. 1, pp. 3 – 4, 2004.

[6] V. Chrisitianto and F. Smarandachey, “A derivation of Maxwell equations in quaternion space,” Progress in Physics, vol. 2, pp. 23 – 27, 2010.

[7] D. Holm. (2011) Geometric mechanics, part ii: Rotating, translating and rolling. [Online]. Available: http://wwwf.imperial.ac.uk/∼dholm/classnotes/GeomMech2-2nd.pdf

[8] D. B. Sweetser. (2005) Doing physics with quaternions. [Online]. Available: http://www.theworld.com/∼sweetser/ quaternions/ps/book.pdf

[9] A. Waser. (2001) Quaternions in electrodynamics. [Online]. Available: http://hotstreamer.deanostoybox.com/temp/QuaternionsInElectrodynamicsEN02.pdf

[10] P. Berner. (2008) Technical Concepts - Orientation, Rotation, Velocity and Acceleration, and the SRM. [Online]. Available: http://www.sedris.org/wg8home/Documents/WG80485.pdf

[11] C. C. Took and D. P. Mandic, “The quaternion lms algorithm for adaptive filtering of hypercomplex processes,” IEEE Trans. Signal Process., vol. 57, no. 4, pp. 1316–1327, 2009.

[12] C. Jahanchahi, C. C. Took, and D. P. Mandic, “A class of quaternion-valued affine projection algorithms,” Signal Process., no. 93, p. 1712–1723, 2013.

[13] X. Gou, Z. Liu, and Y. Xu, “Biquaternion cumulant-music for doa estimation of noncircular signals,” Signal Process., vol. 93, pp. 874 – 881, 2013.

[14] X. Zhang, W. Liu, Y. Xu, and Z. Liu, “Quaternion-valued robust adaptive beamformer for electromagnetic vector-sensor arrays with worst-case constraint,” Signal Process., vol. 104, pp. 274 – 283, 2014.

[15] J. Navarro-Moreno, R. M. Fernandez-Alcal, C. Took, and D. P. Mandic, “Prediction of wide-sense stationary quaternion random signals,” Signal Process., vol. 93, pp. 2573 – 2580, 2013.

[16] F. Ortolani, D. Comminiello, M. Scarpiniti, and A. Uncini, “Frequency domain quaternion adaptive filters: Algorithms and convergence performance,” Signal Processing, vol. 136, pp. 69– 80, Jul. 2017.

[17] F. Ortolani, M. Scarpiniti, D. Comminiello, and A. Uncini, “On 4-dimensional hypercomplex algebras in adaptive signal processing,” in 27th Italian Workshop on Neural Networks (WIRN), Jun. 2017.

[18] S. Smith, “The four-dimensional Sklyanin algebras,” K-Theory, vol. 8, pp. 65–80, 1994.

[19] S. Said, N. L. Bihan, and S. J. Sangwine, “Fast complexified quaternion Fourier transform,” IEEE Trans. Signal Process., vol. 56, no. 4, pp. 1522 – 1531, 2008.

[20] M. A. Gerzon, “Ambisonics in multichannel broadcasting and video,” J. Audio Eng. Soc., vol. 33, no. 11, p. 859871, 1985.

[21] M. A. Gerzon, “Ambisonics. Part two: Studio techniques,” Studio Sound, vol. 17, pp. 24–26, 28–30, 1975.

[22] P. Fellgett, “Ambisonics. part one: General system description,” Studio Sound, vol. 17, pp. 20–22, 1975.

[23] F. Rumsey, Spatial Audio. Focal Press, 2001.

[24] J. Daniel, R. Nicol, and S. Moreau, “Further investigations of high order ambisonics and wavefield synthesis for holophonic sound imaging,” in AES 114th Conv., Mar. 2003.

[25] F. Ortolani, M. Scarpiniti, D. Comminiello, and A. Uncini, “Advances in hypercomplex adaptive filtering for 3d audio processing,” in IEEE First Ukraine Conference on Electrical and Computer Engineering (UKRCON), May 2017.

[26] F. Ortolani and A. Uncini, “A new approach to acoustic beamforming from virtual microphones based on Ambisonics for adaptive noise cancelling,” in IEEE 36th Int. Conf. on Electronics and Nanotechnology (ELNANO), Apr. 2016.